Modification of Brittle Polylactide by Novel Hyperbranched Polymer-Based Nanostructures

Rahul Bhardwaj and Amar K. Mohanty*

School of Packaging, Michigan State University, 130 Packaging Building, East Lansing, Michigan 48824

Received April 3, 2007; Revised Manuscript Received May 20, 2007

The inherent brittleness of polylactide (PLA) poses considerable scientific challenges and limits its large-scale applications. Here, we propose and demonstrate a new industrially relevant methodology to develop a polylactide (PLA)-based nanoblend having outstanding stiffness−toughness balance. In this approach, a hydroxyl functional hyperbranched polymer (HBP) was in-situ cross-linked with a polyanhydride (PA) in the PLA matrix during melt processing. There was formation of new hyperbranched polymer-based cross-linked particles in the PLA matrix. Transmission electron microscopy (TEM) and atomic force microscopy (AFM) revealed the sea-island morphology of PLA-cross-linked HBP blend. The domain size of cross-linked HBP particles in the PLA matrix was less than 100 nm as obtained from TEM. The presence of cross-linked hyperbranched polymer in the PLA matrix exhibited ∼570% and ∼847% improvement in the toughness and elongation at break, respectively, as compared to unmodified PLA. The increase in the ductility of modified PLA was related to stress whitening and multiple crazing initiated in the presence of cross-linked HBP particles. Formation of a networked interface as revealed by rheological data was associated with enhanced compatibility of the PLA-cross-linked HBP blend as compared to the PLA/HBP blend. The cross-linking reaction of HBP with PA was confirmed with the help of Fourier transform infrared spectroscopy (FTIR) and low-temperature dynamical mechanical thermal analysis (DMTA).

1. Introduction

There is an increased emphasis on the enhancement of material properties with the structures engineered at nanometer length scales. The inherently high surface-area−volume ratio of nanometer-sized materials plays a key role in enhancing the desired properties. Recently, nanostructure polymer blends having a minority polymer phase with nanoscale dimensions offered much promise because of enhanced thermomechanical properties, optical transparency, and toughness in comparison to conventional polymer blends. Reactive blending, utilizing the concept of in-situ polymerization, and graft and block copolymerization lead to the creation of nanostructure blends.[1,2] So far the nanostructure blending is restricted to a handful of petroleum-based polymers, i.e., polyamide (PA), polypropylene (PP), and poly(vinylidene fluoride) (PVDF).[1−3] In the midst of these polymers, polylactide (PLA) or polylactic acid is emerging as a promising thermoplastic polyester because of its renewable resource-based origin along with its biodegradability and biocompatibility.[4] PLA can exist in three stereochemical forms: poly(L-lactide) (PLLA), poly(D-lactide) (PDLA), and poly(DL-lactide) (PDLLA).[5] The inherent brittleness of PLA has been a major bottleneck for its large-scale commercial applications. Numerous approaches such as plasticization, block copolymerization, blending with tough polymers, and rubber toughening have been adopted to improve the toughness of brittle polylactide bioplastic.[6−9] The major drawbacks of these methods are the substantial decreases in the strength and modulus of the toughened polylactide. So, a polylactide-based material having good stiffness−toughness balance along with high biobased polylactide content is still elusive.

Previous research suggested that the brittleness of PLA is due to the low entanglement density (V_e) and the high value of characteristic ratio (C_∞), a measure of chain stiffness.[10−12] The enantiomerically pure PLAs, such as PLLA and PDLA as well as amorphous PLA, deform in a brittle fashion because of the formation of crazes.[13] Crazes are the microcracks bridged by small fibrils and often lead to the catastrophic failure of a polymer. In conventional polymers, polystyrene (PS) is a classical example of a craze-forming polymer.[14] Micron-scale rubber particles are usually dispersed in the PS matrix to enhance its toughness. In conventional rubber toughening, some of the major drawbacks are incompatibility between rubber particles and the polymer phase, high shear processing, and increased melt viscosity.

In the midst of polymers having conventional molecular architecture such as linear, branched, and cross-linked, hyperbranched polymers (HBP) are the emerging additives, which fall in the category of dendritic polymers and are gaining attention because of their unique structures and properties. Hyperbranched polymers encompass highly branched nanoscopic structures having high peripheral functionalities.[15] They are polydisperse and can be prepared in a one-pot synthesis unlike dendrimers, making the former less costly. The role of hyperbranched polymers is reported as processing aids, branching agents, compatibilizers, and toughners for conventional thermoplastics and thermosets.[16−19] However, the unique physical properties and high peripheral functionalities of HBP offer many other pathways for polymer modification. HBP can play a role of novel building blocks for generating new nanostructures inside a polymer matrix ranging from core−shell to highly networked morphologies. In our recent findings,[20] cross-linking of hydroxyl functional hyperbranched polyesters in the PLA matrix is demonstrated as a new method to overcome its brittleness, and the modified PLA showed promise in various applications.

In this paper, we report the creation of a novel polylactide (PLA)-based nanoblend by in-situ generation of new hyper-

* Author to whom correspondence should be addressed. E-mail: mohantya@msu.edu, phone: +1-517-355-3603.

10.1021/bm070367x CCC: $37.00
Published on Web 07/03/2007

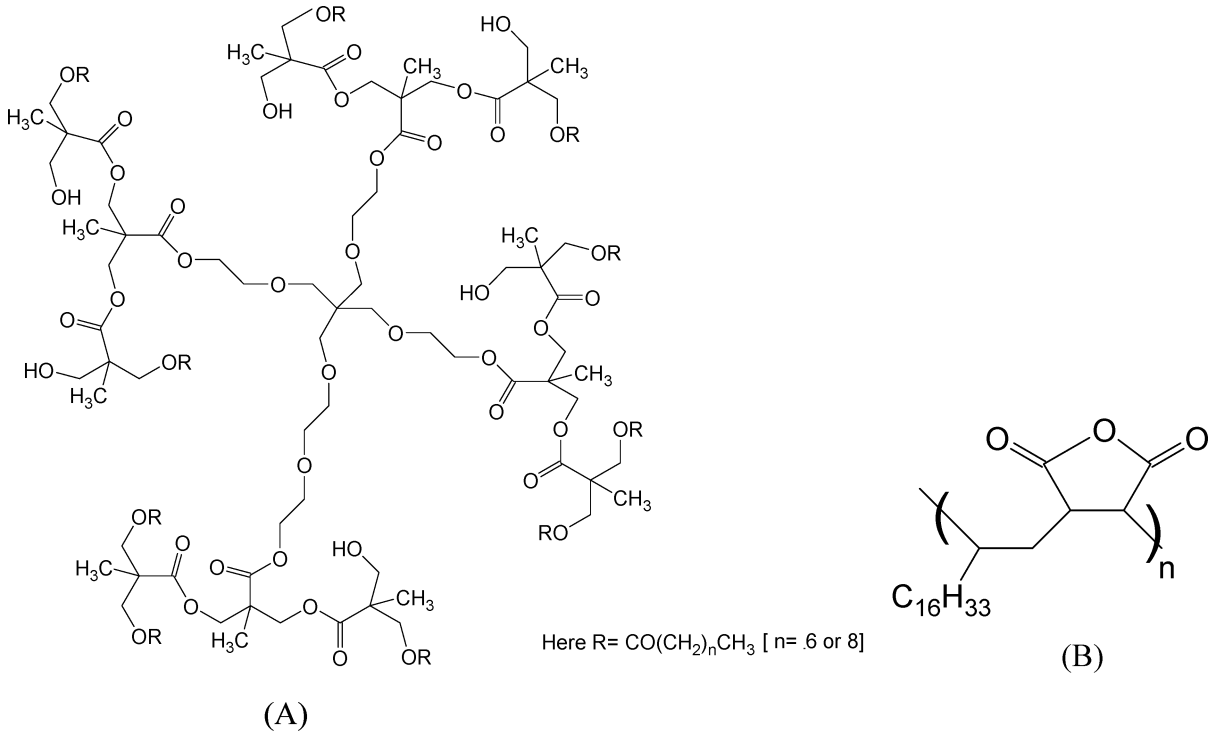

Figure 1. (A) Chemical structure of the chief constituent of hyperbranched polymer (HBP). (B) Chemical structure of polyanhydride (PA).

branched polymer (HBP)-based nanostructures in the matrix polymer prepared via an environmentally friendly melt processing technique. Fourier transform infrared spectroscopy (FTIR), low-temperature dynamical mechanical thermal analysis (DMTA), parallel plate rheology, transmission electron microscopy (TEM), atomic force microscopy (AFM), tensile testing, and scanning electron microscopy (SEM) were used to characterize the blends.

2. Experimental Section

2.1. Materials. Poly(lactic acid), PLA (Biomer L9000) (mol. wt.: 188 kDa from GPC) was obtained from Biomer, Germany. The PLA was the L-form of poly(lactic acid). The hyperbranched polymer (HBP), a dendritic polymer having the trade name BOLTORN H2004, mol. wt. 3200 g/mol was procured from Perstorp (Perstorp, Sweden). BOLTORN H2004 has six primary hydroxyl groups, with a hydroxyl value of 110−135 mg KOH/g and maximum acid number of 7 mg KOH/g. Polyanhydride, trade name PA-18 (LV), having an average molecular weight ~ 22500 g/mol was obtained from Chevron-Phillips, The Woodlands, Texas, USA. The PA is a linear polyanhydride resin having a 1:1 mole ratio of 1-octadecene and maleic anhydride.

2.2. Reactive Extrusion. The PLA was dried for 4 h at 40 °C in a vacuum oven before processing. The HBP was dried for 4 h at 80 °C in a convection oven. The blends were prepared by melt mixing in a microcompounder/microextruder (DSM Research, Netherlands). The instrument is a corotating twin-screw microcompounder having a screw length of 150 mm, L/D of 18, and barrel volume of 15 cm^3. The test specimens were prepared with the help of a mini-injection molder. All compositions made were on weight/weight basis. Initially, PLA was melted in the microcompounder. The hyperbranched polymer (HBP) was added, followed by addition of an appropriate amount of polyanhydride (PA). The chemical structures of the polyanhydride (PA) and the chief constituent of HBP are depicted in Figure 1.[21,22] The hyperbranched polymer was a second generation of dendritic aliphatic polyester having alkyl and hydroxyl groups at the periphery. It was synthesized from an AB2 type monomer and a B4 type core. The hyperbranched polyester was based on 2,2-bis-methylolpropionic acid (bis-MPA) as a chain extender with a pentaerythritol derivative core. There were six primary hydroxyl groups (OH) groups at the periphery of this HBP. The glass transition temperature (T_g) of the HBP was around −40 °C. A multifunctional polyanhydride (PA) was selected as a cross-linking agent for the hyperbranched polymer. PA was a copolymer of octadecene and maleic anhydride having a 1:1 molar ratio. The hydroxyl functionality of HBP was exploited to cause an interparticle cross-linking of HBP to obtain new highly networked morphologies inside the PLA matrix. The reactivity of hydroxyl (OH) functional compounds with anhydride groups containing copolymer is well-known.[23] The molar ratio of hydroxyl (OH) to anhydride group was 1:2. The molar ratio was calculated on the basis of hydroxyl and anhydride equivalent weight of hyperbranched polymer (HBP) and polyanhydride (PA), respectively. Figure 2 schematically depicts the in-situ cross-linking of HBP with PA in the PLA matrix performed during melt processing of PLA. The details of processing parameters and material types are given in Table 1. The processing cycle time of different blends were obtained by observing the variation of the extruder force with cycle time. Here the cycle time represents the duration of time used for the mixing of polymers after material feeding and before removal of material from the microcompounder. In the case of neat PLA, the extruder force increased until the PLA pellets melted and then dropped with the cycle time. For the PLA/HBP (92/08) blend, the force remarkably dropped because of the lubricating effect of HBP and the decrease in the melt viscosity of PLA in the presence of HBP. The addition of polyanhydride (PA) to the PLA/HBP system caused the extruder force to increase with cycle time and stabilized around 10 min of cycle time. This cycle time represented the time for which PLA, HBP, and PA were mixed in microcompounder at a screw speed of 100 rpm. The overall composition for this blend was PLA/HBP/PA (92/5.4/2.6). The increase in the extruder force was attributed to the cross-linking reaction of HBP with PA in the PLA matrix. A control sample of the PLA/PA (97.3/2.7) blend was also fabricated at the same processing condition like that of the PLA/HBP/PA (92/5.4/2.6) blend. The blend had a similar ratio of PLA to PA concentration as it was in the PLA/HBP/PA blend. The purpose of this blend was to investigate the possible interaction of PA with PLA and its effect on the resulting properties of PLA.

2.3. Testing and Characterization. Solvent extraction and ultracentrifugation technique were used to determine the insoluble compo-

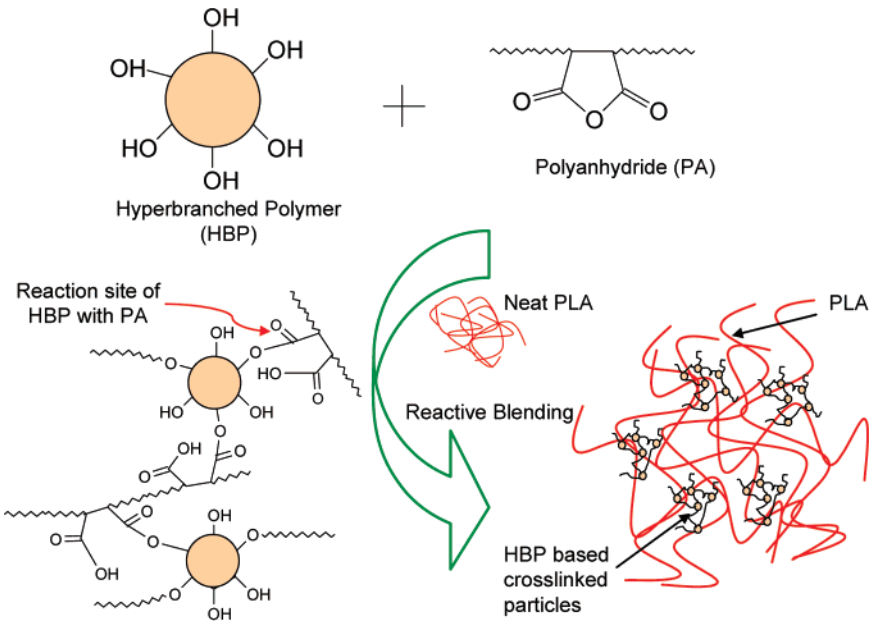

Figure 2. Schematic illustrations of in-situ cross-linking of hyperbranched polymer (HBP) in the PLA melt with the help of a polyanhydride (PA).

Table 1. Processing Parameters of Neat PLA and Its Blends

material compositions (wt. %/wt. %)	processing temp (°C) at three zones of miniextruder			cycle time (min)
	Top	center	bottom	
neat PLA	185	185	185	3
PLA/HBP (92/08)	185	185	185	3
PLA/HBP/PA (92/5.4/2.6)	185	185	185	10
PLA/PA (97.3/2.7)	185	185	185	10

nent in neat PLA and its blends. The 0.5 g of processed blends were dissolved in 30 mL of methylene dichloride (CH_2Cl_2) (Jade Scientific) and stirred for 4 h at room temperature. The solutions were observed for their physical appearance. The insoluble fraction of the PLA/HBP/PA (92/5.4/2.6) blend was extracted with repeated cycles of centrifugation (3000 rpm, 30 min) and solvent wash. The insoluble fraction was dried for 24 h at 40 °C and characterized with scanning electron microscopy (SEM). The chemical composition of the insoluble fraction was evaluated with help of a Perkin-Elmer system 2000 FTIR spectrometer having ATR assembly. The weight fraction of the insoluble cross-linked HBP particles formed by the reaction of HBP and PA was calculated by following equation:

$$W_{\mathrm{cHBP}} = \frac{W_{\mathrm{ins}}}{W_{\mathrm{HBP}} + W_{\mathrm{PA}}} \qquad (1)$$

where W_{cHBP} = weight fraction of cross-linked HBP particles, W_{ins} = final weight of insoluble fraction after extraction and drying, W_{HBP} = initial weight of HBP in PLA composition, and W_{PA} = initial weight of PA in PLA composition.

The dynamical mechanical thermal analysis (DMTA) of the neat PLA and its blends were performed with DMA Q800, TA Instruments, New Castle, Delaware, USA. The test was carried out at a heating rate of 3 °C/min from −90 to 150 °C in the single cantilever mode. The drive amplitude was 15 μm, while the oscillating frequency was 1 Hz. Rheological studies of neat PLA and its blends were conducted with an ARES parallel plate rheometer in dynamic strain frequency sweep mode. The plates had 25 mm diameter. The gap between plates was 0.5 mm during testing. The test was conducted in the frequency range of 0.1 to 100 rad/s at a strain rate of 1% and at a testing temperature of 175 °C. A transmission electron microscope (TEM) (JEOL 100 CX)

Table 2. Behavior of PLA and Its Blends after Dissolving in Methylene Dichloride

material compositions (wt. %/wt. %)	appearance
neat PLA	clear
PLA/HBP (92/08)	clear
PLA/HBP/PA (92:5.4:2.6)	Turbid
PLA/PA (97.3/2.7)	Clear

was used to analyze the morphology of PLA-based blends at an accelerating voltage of 100 kV. Microtomed ultrathin film specimens with thickness of less than 100 nm were used for TEM observation. The microtomy was carried out at room temperature using a diamond blade on a RMC microtome station. The PLA-based blend samples were stained with ruthenium tetroxide (RuO_4) before examination. Atomic force microscopy (AFM) of microtomed surface of modified PLA was performed on a AFM microscope (Digital Instrument MultiMode SPM with Nanoscope IV controller, Digital Instruments, NY) in tapping mode. Scan sizes of 10 and 5 μm at a scan rate of 0.5044 Hz were used for AFM analysis. Contrast enhancement of AFM pictures was also performed. Tensile properties of neat PLA and its blends were measured using a United Calibration Corp SFM 20 testing machine as per ASTM D638. The specimens having a gage length of 2.54 mm were tested at a cross-head speed of 15.4 mm/mm-min. A JEOL scanning electron microscope (model JSM-6400) was used to evaluate the morphology of tensile-fractured surfaces of the neat PLA and its blends. An accelerating voltage of 15 kV was used to produce the SEM photomicrographs.

3. Results and Discussion

3.1. Solvent Extraction, Morphology, and Fourier Transform Infrared Spectroscopy. The physical observation of the solutions of PLA and its blends in methylene dichloride are depicted in Table 2. All of the solutions were clear in appearance except that of the PLA/HBP/PA (92/5.4/2.6) blend, which was turbid in appearance. The turbidity was attributed to the scattering of light by the suspended particles in continuous PLA solution. Methylene dichloride is a reported as good solvent for PLA.[24] So it was likely that the particles were the reaction product of HBP and PA. The reaction of HBP and PA could

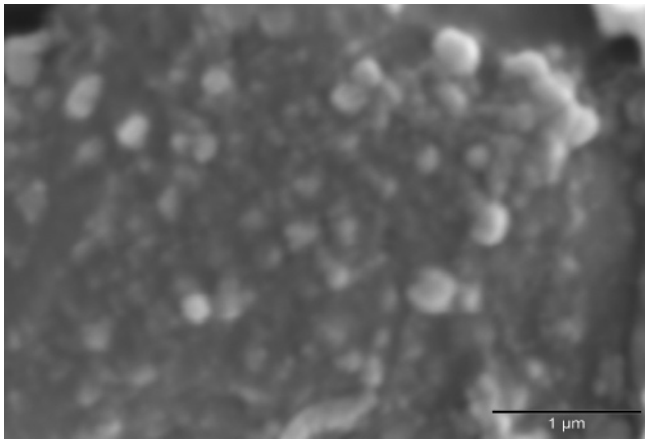

Figure 3. SEM photomicrographs of extracted cross-linked HBP particles from the PLA matrix.

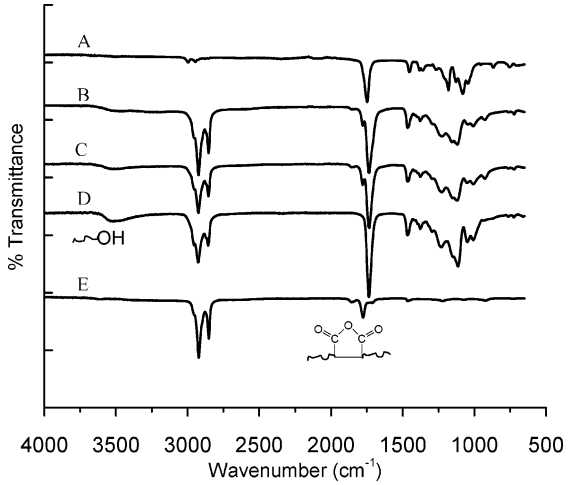

Figure 4. FTIR spectrum: A: Neat PLA; B: HBP/PA particles (extracted), C: HBP/PA particles (outside); D: Hyperbranched polymer (HBP); E: polyanhydride (PA).

form cross-linked network because of their multifunctionality and make them insoluble in a solvent. The insoluble mass was dried and characterized with SEM and FTIR. The scanning electron microscopy (Figure 3) of extracted cross-linked HBP revealed particle morphology of the extracted insoluble fraction. The particles were fused with each other after solvent removal. Most of these particles had dimensions less than 100 nm. The photomicrograph also revealed large size distribution of cross-linked particles. In order to confirm the reaction of HBP with PA, HBP was allowed to react with polyanhydride (PA) in a laboratory flask in the absence of PLA for 10 min at 185 °C. The molar ratio of OH to anhydride was 1:2. There was gelation and formation of a solid mass as a result of the reaction between HBP and PA. Figure 4 represents the FTIR spectrum of PLA, HBP/PA particles (extracted), HBP/PA particles (reacted outside), neat HBP, and PA. The FTIR spectrum of extracted particles showed a spectrum having similar peaks like that of HBP and PA. There was strong reduction in the broadness and intensity of OH peaks (3600−3500 cm^{-1}) in the spectra of extracted particles. On the other hand, the FTIR spectra of neat HBP showed strong absorption in this region due to the presence of primary hydroxyl groups in its structure. The broadness in the peak for HBP was due to the presence of inter- as well as intramolecular hydrogen bonding in HBP. The interpretation of hydroxyl peaks suggested that the OH groups of HBP had been reacted with anhydride group of PA and formed monoester. There was the presence of two characteristic anhydride frequency bands at 1855 and 1777 cm^{-1} in extracted HBP/PA particles due to the coupled vibration of symmetric and asymmetric stretching of two >C═O groups in the anhydride group of a polyanhydride. These bands accounted for the presence of unreacted anhydride groups in the extracted particles. The molar ratio of OH to anhydride was 1:2 in the PLA/HBP/PA blend so it was quite expected that there would be the presence of a free anhydride group. The characteristic anhydride frequency bands of extracted particles matched perfectly with that of the polyanhydride (PA). The fingerprint region (<1500 cm^{-1}) of the spectra of extracted particles was in coherence with that of HBP. There was no presence of characteristic bands of PLA in the spectra of extracted particles. This suggested that the main reaction occurred between HBP and PA in the PLA matrix, while the PLA chains were physically entangled in the network of HBP and PA. PLA has functional groups (OH and COOH) only at the chain ends, which might not able to react with the OH and anhydride group of HBP and PA, respectively. A further confirmation of the reaction of HBP with PA in the PLA matrix was performed by comparing the FTIR spectra of the reaction product of HBP and PA in the absence of PLA. The FTIR spectra of extracted particles were in complete unison with that of particles prepared outside (Figure 4B and C). This result confirmed that the polyanhydride had successfully caused the cross-linking of HBP in the PLA matrix. The weight fraction of extracted cross-linked HBP particle was calculated as per eq 1 and was ∼0.89, i.e., 89%. So there was high reactivity of HBP with PA in the PLA matrix. The presence of some unreacted HBP and PA was primarily due to steric hindrance created by a large amount of PLA media.

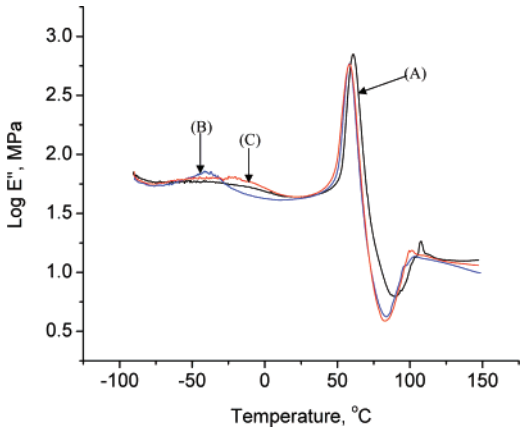

Figure 5. Temperature dependence of the loss modulus (E'') of (A) neat PLA, (B) PLA/HBP (92/08) blend, and (C) PLA/HBP/PA (92/5.4/2.6) blend. The shift in the glass transition temperature (T_g) of HBP from −40 °C to −31 °C indicated the occurrence of cross-linking of the HBP.

3.2. Dynamical Mechanical Thermal Analysis. Low-temperature dynamical mechanical thermal analysis (DMTA) was conducted to observe the cross-linking of HBP, phase separation, and molecular interaction of PLA with HBP and cross-linked HBP (cHBP). The temperature dependency of loss modulus (E'') of neat PLA, PLA/HBP (92/08) blend, and PLA/HBP/PA (92/5.4/2.6) blend is shown in Figure 5. In the PLA/HBP (92/08) blend, there were two loss modulus (E'') relaxation peaks at −40 °C and 58 °C, respectively, corresponding to the glass transition temperature (T_g) of HBP and PLA, respectively. There was slight depression in the T_g of PLA in the presence of HBP. It suggested that there was some molecular interaction between PLA and HBP, but this system was dominated by phase separation. Phase separation has also been a major problem in

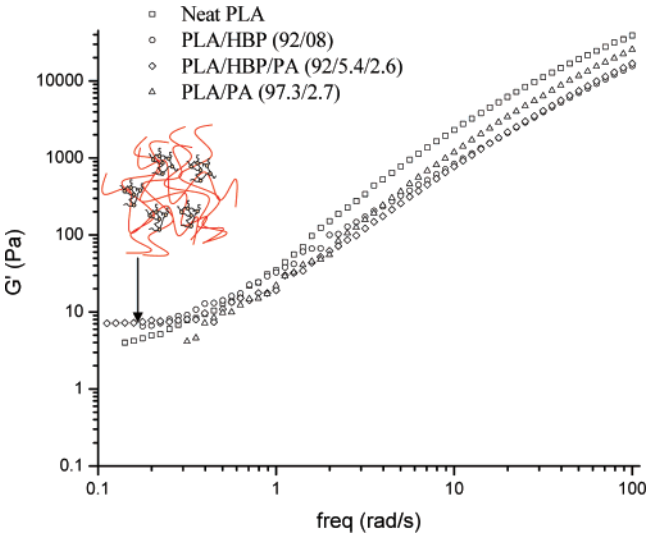

Figure 6. Behavior of storage modulus, G', of neat PLA and its blend as a function of oscillatory frequency (ω).

most of the plasticized PLA systems.[25] The creation of free volume in plasticized PLA enhances its molecular mobility, facilitating the increase in its crystallinity, which renders the expulsion of plasticizer molecules from the amorphous region.

On the other hand, the PLA/HBP/PA (92/5.4/2.6) composition revealed two peaks at −31 °C and 58 °C, representing the glass transition temperature (T_g) of cross-linked HBP (cHBP) and PLA, respectively. There was a shift in glass transition temperature from −40 °C for HBP in the PLA/HBP blend to −31 °C for cHBP in PLA/HBP/PA blend. This suggested that polyanhydride (PA) had selectively caused the cross-linking of HBP in the PLA matrix. The increase in the glass transition temperature of cross-linked HBP was attributed to the restricted segmental mobility and increase in the molecular weight of HBP after cross-linking. In theory, cross-linking would increase the Flory−Huggin interaction parameter and thus would aggravate the phase instability.[26] It was also demonstrated that cross-linking helped in inhibiting the macrophase separation.[27] The phase stability of a system in which one species is cross-linked is dictated by the entropic interaction. The fractal dimension of these cross-linked HBP would be responsible for new entropic interactions. The present system could be considered as a pseudo-semi-interpenetrating network system. Here, in the presence of a linear PLA chain, the hyperbranched polymer was cross-linked, thus leading to the formation of highly branched networked domains in the PLA matrix. The growing network of HBP during the in-situ reaction could cause physical interlocking with PLA chains thus helping to reduce the macrophase separation of HBP from the PLA phase. It was likely that physical interlocking of PLA chain with the growing network of HBP occurred at the phase boundaries between PLA and cross-linked HBP only, primarily because of the limited miscibility of PLA with HBP.

3.3. Rheological Evidence of Networked Interface between PLA and Crosslinked HBP. The variation of the storage modulus, G', with small-amplitude oscillatory frequency for the neat PLA and its blends is given in Figure 6. There was a distinct formation of a rubbery plateau of highest length in the case of the PLA/HBP/PA (92/5.4/2.6) blend unlike that of neat PLA, the PLA/HBP (92/08) blend, and the PLA/PA (97.3/2.7) blend in lower frequency region. The formation of a rubbery plateau is determined by the presence of cross-links and entanglement in a polymer.[28] When observing the lowest frequency region of all curves, it was found that the PLA/HBP/PA (92/5.4/2.6) blend had highest value of plateau modulus. Such an increase in plateau modulus is caused by the presence of cross-links or entangled networks in a polymer melt.[28] So it was believed that the presence of the cross-linked HBP network caused the upward shift in the plateau modulus. On the other hand, the in-situ cross-linking of HBP with PA in the PLA melt caused the formation of cross-linked particles, which had the tendency to form an entangled network with the PLA chain preferably at the interface. The terminal slope of the $G'-\omega$ curve approached zero for the PLA/HBP/PA (92/5.4/2.6) system, reflecting its pseudo-solid-like behavior. The relaxation and motion of the PLA chain, which was a major fraction in the blend, would have a prominent effect on rheological properties in low shear regime. The longer relaxation of the PLA chain in the presence HBP/PA particles caused the frequency independence of storage modulus in lower shear regime. This behavior also strongly indicated toward formation of a physical network of the PLA chains with HBP/PA particles during their in-situ reaction in the PLA matrix.

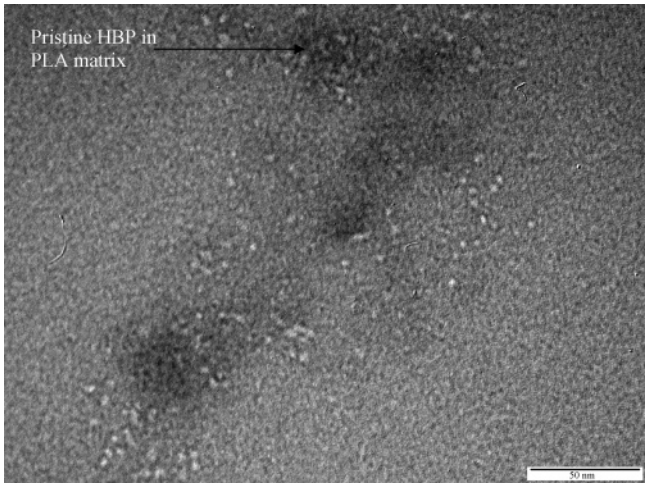

Figure 7. Transmission electron micrographs of PLA having 8 wt.% of pristine HBP. (Scale bar: 50 nm).

3.4. Transmission Electron Microscopy (TEM). Transmission electron microscopy (TEM) was carried out to evaluate the morphology and dispersion of pristine and cross-linked HBP particles in the PLA matrix. The ultramicrotomed samples of the PLA/HBP (92/08) and PLA/HBP/PA (92/5.4/2.6) blends were stained with ruthenium tetroxide (RuO_4) before TEM observation. Ruthenium tetroxide selectively stained the ether moiety present in the hyperbranched polymer and appeared darker than the PLA phase in the TEM photomicrographs. The TEM photomicrograph (Figure 7) of the PLA /HBP (92/08) blend revealed the nanoscopic dimension of HBP (4−6 nm), but they were not well distributed in the PLA matrix and appeared rather as discrete agglomerations. This was attributed to the limited miscibility of HBP with PLA and the presence of strong intermolecular hydrogen bonding between HBP molecules due to their high peripheral hydroxyl functionalities. Figure 8A and 8B revealed the nanoscale phase-separated sea-island morphologies of the PLA/HBP/PA (92/5.4/2.6) blend, in which cross-linked HBP particles (dark patches) had various size orders, having dimensions ranging from 50 to 100 nm. There was heterogeneous size distribution of cross-linked HBP particles in the PLA matrix. The multifunctionalities of HBP and PA and random effective collisions of HBP molecules with PA molecules during their reaction in the large sea of PLA were the possible reasons behind the random size distribution. The heterogeneity in the morphologies of cross-linked HBP particles

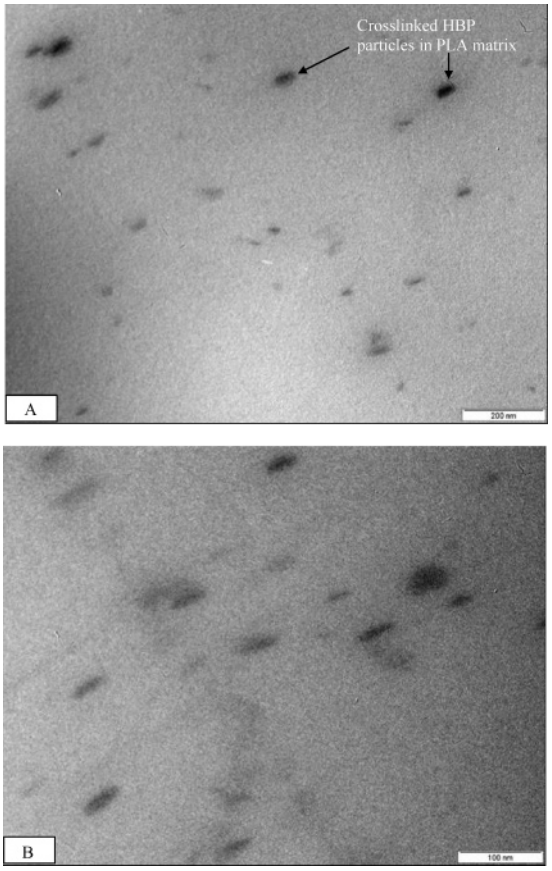

Figure 8. Transmission electron micrographs of PLA having cross-linked HBP. A: Scale bar: 200 nm; B: Scale bar: 100 nm.

would also arise from the polydispersity of pristine HBP itself and the uncontrolled cross-linking reaction. The variation in stain intensity of cross-linked HBP particles also indicated the random cross-linking of HBP particles. The phase boundaries of all of the cross-linked particles were diffused and devoid of any sharp demarcation, which was an indication toward formation of a network between PLA and cross-linked HBP chains. Such networked structures at an interface would increase the compatibility between two phases.

3.5. Atomic Force Microscopy (AFM). Further confirmation of the formation of HBP-based nanoscale particles in modified PLA was obtained by tapping mode atomic force microscopy (TM-AFM) analysis. There was clear evidence of formation of nanoscale morphologies in the PLA/HBP/PA (92/5.4/2.6) blend in the phase images (Figure 9A,B). The difference in the viscoelastic behavior of two phases present in the sample caused a phase lag, which led to appearance of contrast in the AFM image.[29] The lighter area corresponds to the soft cross-linked HBP phase while the darker area was due to the stiff PLA phase. There was heterogeneity in the dispersed phase morphology that correlated well with the TEM images. The dispersed phase dimensions from AFM were in the range of 80−200 nm. The difference in the dispersed phase size from AFM and TEM micrographs was obvious, as the tip radii, scan rate, and scan size affect the resolution in AFM. Another major difference was in the appearance of a lesser number of particles in AFM pictures than in TEM pictures. The AFM was carried out in tapping mode over a smooth surface of modified PLA. There was probability that some particles might not be exposed to the surface of the scanned area. On the other hand, a thin cross-section (∼70 nm) of modified PLA was stained with ruthenium tetroxide and examined under an electron microscope. So, it

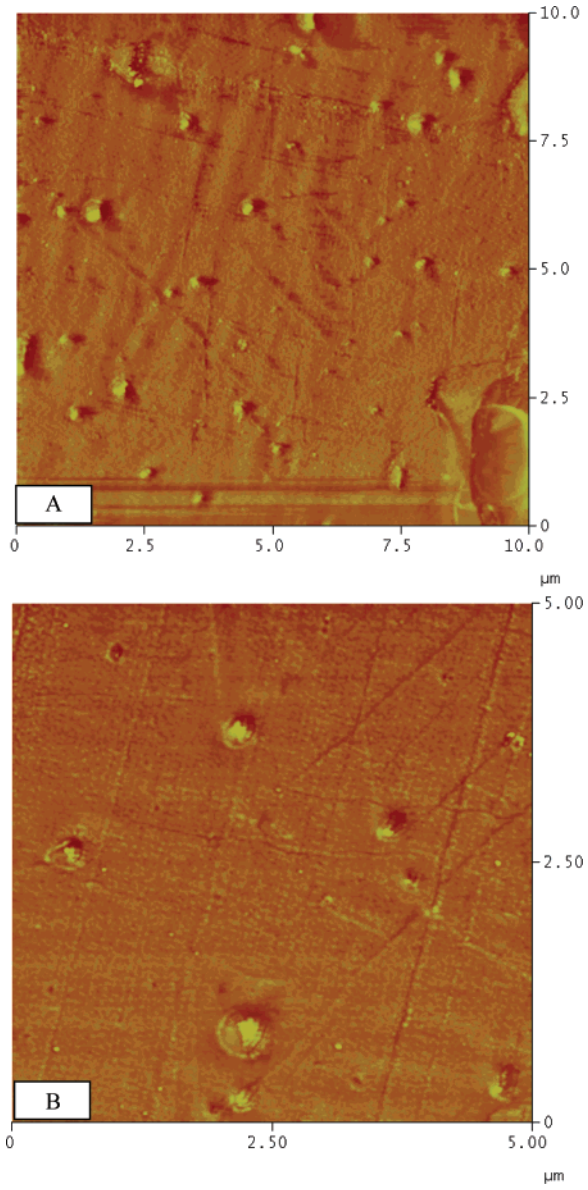

Figure 9. Tapping mode AFM phase image of the PLA/HBP/PA (92/5.4/2.6) blend revealed nanoscale domains of cross-linked HBP particles in the continuous PLA matrix. A: Scan size: 10 μm; B: Scan size: 5 μm.

was possible to spot these stained cross-linked HBP particles more easily. Thus, the TEM can estimate a larger population of particles and their sizes more accurately than AFM for this sample. The purpose of characterizing modified PLA with AFM was to validate the two-phase morphology of modified PLA and the softer nature of cross-linked HBP particles. The presence of depressions around cross-linked HBP particles in AFM images was a microtomy artifact. The knife cut the softer cross-linked HBP particle deeper as compared to the surrounding stiff PLA matrix and a left a depression.

3.6. Tensile Properties. Stress−strain curves of neat PLA, PLA/HBP (92/08), and PLA/HBP/PA (92/5.4/2.6) blends are shown in Figure 10, while the detail of the measured tensile properties is provided in Table 3. There was no improvement of elongation at break value of PLA when blended with 8 wt.% of pristine HBP as well as with 2.7 wt.% of PA, but the elongation at break of PLA was improved by around ∼847% for the PLA/HBP/PA (92/5.4/2.6) blend. The PLA and PLA/HBP (92/08) blends underwent strain softening and deformed in brittle fashion. On the other hand, the PLA/HBP/PA (92/

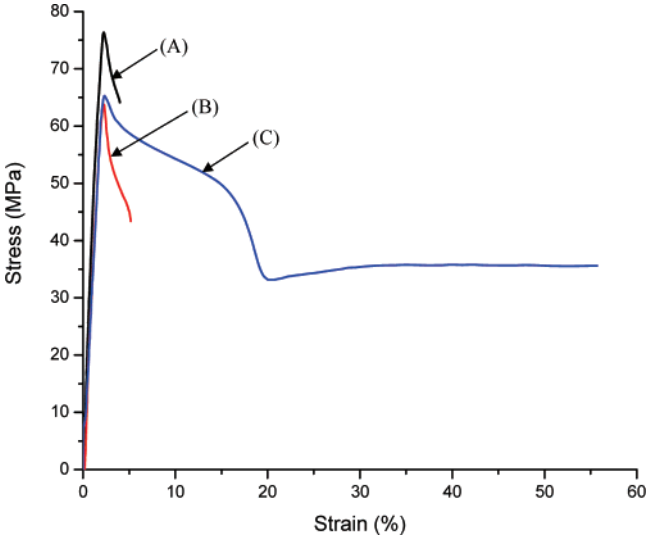

Figure 10. Stress−strain curves obtained at a cross-head speed of 15.4 mm/min: (A) neat PLA; (B) PLA/HBP (92/08); (C) PLA/HBP/PA (92/5.4/2.6).

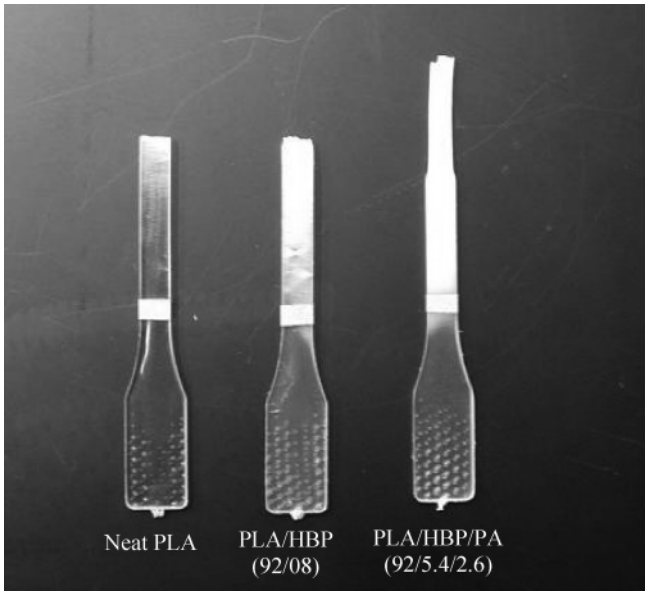

Figure 11. Tensile specimen after testing to failure at 15.4 mm/min under uniaxial tension.

5.4/2.6) blend showed initial strain softening after yielding and then underwent considerable cold drawing. The stress−strain curve after the yield point showed a combination of strain softening and cold drawing. In this region, there was competition between PLA chain orientation and crack formation. Hence, there was a drop in stress with increasing strain. After 20% of strain, only cold drawing dominated at a constant stress. This suggested that a large energy dissipation occurred in the presence of cross-linked HBP particles in the PLA/HBP/PA (92/5.4/2.6) blend. The toughness, calculated as the area under stress−strain, exhibited a drop in its value for the PLA/HBP (92/08) blend as compared to the neat PLA, while increased dramatically from 2.6 MJ/m^3 for neat PLA to 17.4 MJ/m^3 for the PLA/HBP/PA (92/5.4/2.6) blend. This was quite an unusual result, as the modified PLA maintained a quite high tensile modulus value of 2.8 GPa. The result was very significant in obtaining a biobased material having remarkable stiffness−toughness balance. The tensile strength of modified PLA decreased to 63.9 MPa from 76.5 MPa for neat PLA. These results suggested that the nanoscale cross-linked HBP particles behaved like rubber particles and were effective in improving the toughness of PLA at low concentration (8 wt.%) with a minimal sacrifice of tensile strength and modulus. In such a multiphase system, inelastic deformation occurs via the phenomenon of shear yielding, multiple crazing, and cavitation in the softer dispersed phase.[30] PLA is an example of semicrystalline glassy polymer and undergoes brittle deformation via craze formation.[13] The craze volume fraction (V_f) plays a crucial role in determining the propensity of craze for catastrophic failure. The true stress σ_t, acting on the craze fibrils is inversely proportional to the volume fraction of craze, which is given by the equation:[14]

$$\sigma_t = \frac{\sigma_\infty}{v_f} = \lambda\sigma_\infty$$

Here σ_∞ is the applied stress and λ is the craze extension ratio. So increasing the volume fraction of craze can reduce the true stress on an individual craze. Dispersing elastic second phase and plasticization with low molecular weight molecules can provide control over nucleation and growth of crazes and can increase craze plasticity in glassy polymers leading to the decrease in brittleness.[31−34] In the PLA/HBP/PA (92/5.4/2.6) blend, the nanoscale rubbery cross-linked HBP ($T_g \sim -31$ °C) particles were formed in a continuous PLA matrix. During tensile testing, there was stress-whitening in the subfracture region in PLA/HBP (92/08) and PLA/HBP/PA (92/5.4/2.6) blends (Figure 11). The stress whitening was more pronounced in the PLA sample having cross-linked HBP (cHBP) particles, i.e., PLA/HBP/PA (92/5.4/2.6) blend. There was the possibility of the creation of numerous tiny crazes nucleated by cross-linked HBP (cHBP) in the PLA matrix. The stress-whitening occurred because of the scattering of light by these tiny crazes created by cross-linked HBP particles. Such intense stress whitening was absent in the neat PLA sample (Figure 11). So, the phenomenon of multiple crazing was likely the possible energy dissipation mechanism behind the toughening of PLA bioplastic. Here the nanoscale cross-linked particles increased the craze volume fraction and thus reduced the true stress on a single craze. This helped in craze plasticity, leading to the orientation of the PLA chain in load direction. The PLA/HBP (92/08) blend also exhibited stress whitening, but the sample failed in brittle manner. The stability of crazes initiated by the rubbery phase in brittle polymers depends on the level of adhesion between the polymer matrix and dispersed particles. The crazes nucleated by HBP were not stable because of the incompatibility of PLA

Table 3. Mechanical Properties of Neat PLA and Its Blends

materials (wt./wt.)/properties	tensile modulus (Gpa)	tensile strength at yield (MPa)	elongation at break (%)	toughness (MJ/m^3)
PLA (100/00)	3.6 ± 0.07	76.5 ± 1.45	5.1 ± 1.7	2.6 ± 0.9
PLA/HBP (92/08)	3.4 ± 0.05	64.2 ± 0.8	5.1 ± 1.0	1.6 ± 0.7
PLA/HBP/PA (92/5.4/2.6)	2.8 ± 0.2	63.9 ± 1.7	48.3 ± 6.3	17.4 ± 1.5
PLA/PA (97.3/2.7)	2.6 ± 0.1	76.2 ± 0.5	3.3 ± 0.2	1.5 ± 0.6

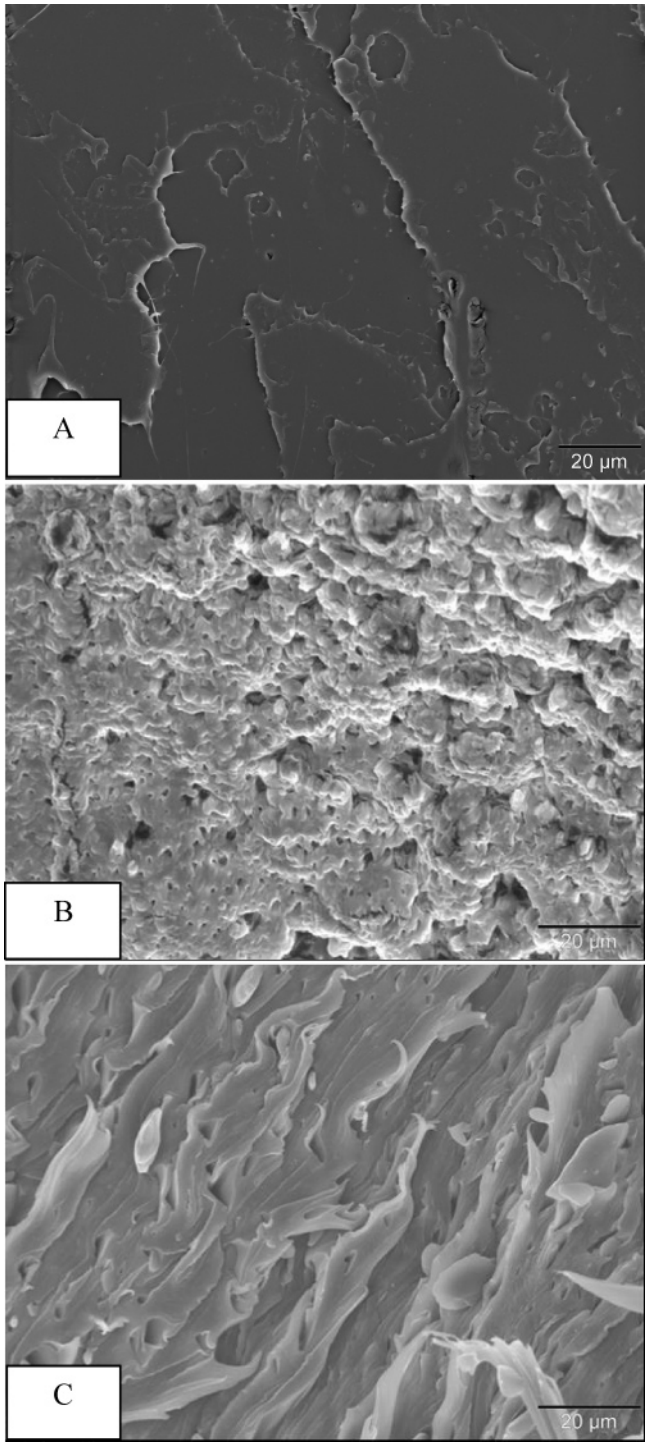

Figure 12. Scanning electron micrographs of tensile fracture surfaces: A: Neat PLA; B: PLA/HBP (92/08); C: PLA/HBP/PA (92/5.4/2.6).

with HBP. In the PLA/HBP (92/08) blend, pristine HBP molecules have strong intermolecular hydrogen-bonding due to their abundant hydroxyl groups, which seems to promoted their aggregation in the PLA matrix and resulted in macroscopic phase separation and inferior properties.

The in-situ reactive blending of HBP and PA in the PLA matrix resulted in the formation of a network at the PLA-HBP interface, which provided the compatibility between the two phases. The creation of numerous stable crazes in the PLA matrix by cross-linked HBP particles helped in the substantial drawing and orientation of PLA chains under tensile loading. The nanoscale dimensions of the cross-linked particle were instrumental in increasing the phenomenon of multiple crazing per unit volume. The increase of the interfacial region due to high surface area of these particles made them effective at lower concentration. The nanoscale particle size tantamount to that of cross-linked HBP is currently not possible using other conventional toughening methodologies.

3.7. Scanning Electron Microscope (SEM). Figure 12 represents the scanning electron micrographs of the tensile fractured surfaces of neat PLA, PLA/HBP (92/08) blend, and PLA/HBP/PA (92/5.4/2.6) blend. The surface of neat PLA was extremely flat, indicating the brittle failure of PLA under tensile loading. The tensile fractured surface of PLA/HBP (92/08) revealed inhomogeniety, formation of voids, and absence of ductile tearing. This was an indication of phase separation, incompatibility between the PLA and HBP, and brittle failure. The in-situ cross-linking of HBP in the PLA matrix dramatically changed its surface characteristic after deformation. The tensile fractured surface of the PLA/HBP/PA (92/5.4/2.6) blend exhibited considerable ductile tearing, surface roughness, and surface integrity. The increased surface area of fractured surface of the PLA/HBP/PA (92/5.4/2.6) blend suggested that the crack paths were highly bifurcated, and crack propagation absorbed considerable strain energy before failure. This led to a conclusion that the in-situ cross-linking of HBP was instrumental in improving the compatibility between the PLA and HBP phase and resulted in significant toughness enhancement of PLA bioplastic.

4. Conclusions

We report that a nanostructure-controlled polylactide (PLA) was created by in-situ cross-linking of hyperbranched polymer (HBP) in the PLA matrix through reactive extrusion blending. The generation of new HBP-based nanostructures in the PLA matrix improved the toughness and elongation at break by ~ 570% and ~847%, respectively, as compared to unmodified PLA. The modified PLA remarkably maintained high strength and modulus values. The cross-linking of HBP was demonstrated by the FTIR analysis and DMTA analysis. The transmission electron microscopy and atomic force microscopy observations of modified PLA confirmed the nanoscopic dimensions of cross-linked HBP particles in the PLA matrix. The scanning electron microscopy analysis clearly exhibited the toughening of PLA. Finally, the current research unwraps the new opportunities available to us from the unique physical and chemical properties of the highly functional hyperbranched polymers in generating new nanostructured multiphase polymer systems with enhanced properties.

Acknowledgment. The financial support of the NSF award DMI-0400296 "PREMISE-II: Design and engineering of green composites from biofibers and bioplastics" is gratefully acknowledged. We are thankful to all our material suppliers. We are indebted to Hazel-Ann Hosein, Composite Material and Structures Center, Michigan State University, and Alicia Pastor, Center for Advanced Microscopy, Michigan State University, for their assistance in the microscopy studies. We are thankful to Edward Drown, Michigan State University, for his comments during the preparation of this manuscript.

References and Notes

(1) Hu, G. H.; Cartier, H. Reactive Extrusion: Toward Nanoblends. *Macromolecules* **1999**, *32*, 4713−4718.

(2) Ruzette, A. V.; Leibler, L. Block copolymers in tomorrow's plastics. *Nat. Mater.* **2005**, *4*, 19−31.
(3) Shimizu, H.; Li, Y.; Kaito, A.; Sano, H. Formation of Nanostructured PVDF/PA11 Blends Using High-Shear Processing. *Macromolecules* **2005**, *38*, 7880−7883.
(4) Ragauskas, A. J.; Williams, C. K.; Davison, B. H.; Britovsek, G.; Cairney, J.; Eckert, C. A.; Frederick, W. J., Jr.; Hallett, J. P.; Leak, D. J.; Liotta, C. L.; Mielenz, J. R.; Murphy, R.; Templer, R.; Tschaplinski, T. The Path Forward for Biofuels and Biomaterials. *Science* **2006**, *311*, 484−489.
(5) Drumright, R. E.; Gruber, P. R.; Henton, D. E. Polylactic Acid Technology. *Adv. Mater.* **2000**, *12* (23), 1841−1846.
(6) Ljungberg, N.; Wesslen, B. Preparation and Properties of Plasticized Poly(lactic acid) Films. *Biomacromolecules* **2005**, *6*, 1789−1796.
(7) Wang, Y.; Hillmyer, M. A. Polyethylene-Poly(L-lactide) Diblock Copolymers: Synthesis and Compatibilization of Poly(L-lactide)/Polyethylene Blends. *J. Polym. Sci. Part A: Polym. Chem.* **2001**, *39*, 2755−2766.
(8) Shibata, M.; Inoue, Y.; Miyoshi, Y. Mechanical properties, morphology, and crystallization behavior of blends of poly(L-lactide) with poly(butylene succinate-co-L-lactate) and poly(butylene succinate). *Polymer* **2006**, *47*, 3557−3564.
(9) Jin, H. J.; Chin, I. J.; Kim, M. N.; Kim, S. H.; Yoon, J. S. Blending of poly(L-lactic acid) with poly(cis-1,4-isoprene). *Eur. Polym. J.* **2000**, *36*, 165−169.
(10) Tonelli, A. E.; Flory, P. J. The Configuration Statistics of Random Poly (lactic acid) Chains. I. Experimental Results. *Macromolecules* **1969**, *2* (3), 225−227.
(11) Joziasse, C. A. P.; Veenstra, H.; Grijpma, D. W.; Pennings, A. J. On the chian stiffness of poly(lactide)s. *Macromol. Chem. Phys.* **1996**, *197*, 2219−2229.
(12) Grijpma, D. W.; Penning, J. P.; Pennings, A. J. Chain entanglement, mechanical properties and drawability of poly(lactide). *Colloid Polym. Sci.* **1994**, *271*, 1068−1081.
(13) Grijpma, D. W.; Pennings, A. J. (Co)polymers of L-lactide, 2a) Mechanical Properties. *Macromol. Chem. Phys.* **1994**, *195*, 1649−1663.
(14) Donald, A. M. In *Physics of glassy polymers*; Harward, R. N., Young, R. J., Eds.; Chapman & Hall: New York, 1997.
(15) Seiler, M. Dendritic Polymers-Interdisciplinary Research and Emerging Applications from Unique Structural Properties. *Chem. Eng. Technol.* **2002**, *25* (3), 237−253.
(16) Hong, Y.; Coombs, S. J.; Cooper-White, J. J.; Mackay, M. E.; Hawker, C. J.; Malmstroḿ, E.; Rehnberg, N. Film blowing of linear low-density polyethylene blended with a novel hyperbranched polymer processing aid. *Polymer* **2000**, *41*, 7705−7713.
(17) Jannerfeldt, G.; Boogh, L.; Manson, J. A. E. Tailored interfacial properties for immiscible polymers by hyperbranched polymers. *Polymer* **2000**, *41*, 7627−7634.
(18) Kil, S. B.; Augros, Y.; Leterrier, Y.; Manson, J. A. E. Rheological Properties of Hyperbranched Polymer/Poly(ethylene Terephthalate) Reactive Blends. *Polym. Eng. Sci.* **2003**, *43* (2), 329−343.
(19) Mezzenga, R.; Boogh, L.; Manson, J. A. E. A review of dendritic hyperbranched polymer as modifiers in epoxy composites. *Compos. Sci. Technol.* **2001**, *61* (5), 787−795.
(20) Mohanty, A. K.; Bhardwaj, R. Hyperbranched polymer modified biopolymers, their biobased materials and process for the preparation thereof. US 20060247387A1 (pending), 2006.
(21) Structure drawn according to *Perstorp Specialty Chemicals, TSCA-Exempted Polymer Structures*; Perstorp Specialty Chemicals: Perstorp, Sweden, Jan 22, 2001.
(22) http://www.cpchem.com/enu/specialty_chemicals_polyanhydride_resins.asp (accessed on February 2, 2007).
(23) Orr, C. A.; Cernohous, J. J.; Guegan, P.; Hirao, A.; Jeon, H. K.; Macosko, C. W. Homogeneous reactive coupling of terminally functional polymers. *Polymer* **2001**, *42* (19), 8171−8178.
(24) Agrawal, A.; Saran, A. D.; Rath, S. S.; Khanna, A. Constrained nonlinear optimization for solubility parameters of poly(lactic acid) and poly(glycolic acid)—validation and comparison. *Polymer* **2004**, *45*, 8603−8612.
(25) Ljungberg, N.; Wesslen, B. The effects of plasticizers on the dynamic mechanical and thermal properties of poly(lactic acid) *J. Appl. Polym. Sci.* **2002**, *86*, 1227−1234.
(26) Mamun, C. K. Free Energy of Mixing of Cross-Linked Polymer Blends, *Langmuir* **2005**, *21*, 240−250.
(27) Klempner, D.; Sperling, L. H.; Utracki, L. A. In *Interpenetrating Polymer Networks*; Advances in Chemistry Series No. 239; American Chemical Society: Washington, DC, 1994.
(28) Edwards, S. F.; Takano, H.; Terentjev, E. M. Dynamic mechanical response of polymer networks. *J. Chem. Phys.* **2000**, *113* (13), 5531−5538.
(29) Sa'nchez, M. S.; Mateo, J. M.; Colomer, J. S. R.; Ribelles, J. L. G. Nanoindentation and tapping mode AFM study of phase separation in poly(ethyl acrylate-co-hydroxyethyl methacrylate) copolymer networks, *Eur. Polym. J.* **2006**, *46*, 1378−1383.
(30) Bucknall, C. B. In *Physics of glassy polymers*; Harward, R. N., Young, R. J., Eds.; Chapman & Hall: New York, 1997.
(31) Bucknall, C. B. *Toughened Plastics*; Applied Science Publications: London, 1977.
(32) Kinloch, A. J.; Young, R. J. *Fracture Behavior of Polymers*; Applied Science Publications: London, 1977.
(33) Gabizlioglu, O. S.; Beckham, H.W.; Argon, A. S.; Cohen, R. E.; Brown, H. R. *Macromolecules* **1990**, *23*, 2968.
(34) Argon, A. S.; Cohen, R. E.; Gabizlioglu, O. S.; Brown, H. R.; Kramer, E. J. *Macromolecules* **1990**, *23*, 3975.

BM070367X